

# MONTE–CARLO SIMULATIONS OF STAR CLUSTERS I. FIRST RESULTS.

Mirek Giersz<sup>1</sup>

<sup>1</sup> *N. Copernicus Astronomical Center, Polish Academy of Sciences, ul. Bartycka 18, 00–716 Warsaw, Poland*

Accepted 199- — -. Received 199- — -; in original form 1996 December 1 — ???

## ABSTRACT

A revision of Stodółkiewicz’s Monte–Carlo code is used to simulate evolution of star clusters. The new method treats each *superstar* as a single star and follows the evolution and motion of all individual stellar objects. The first calculations for isolated, equal–mass  $N$ –body systems with three–body energy generation according to Spitzer’s formulae show good agreement with direct  $N$ –body calculations for  $N = 2000, 4096$  and  $10000$  particles. The density, velocity, mass distributions, energy generation, number of binaries etc. follow the  $N$ –body results. Only the number of escapers is slightly too high compared to  $N$ –body results and there is no level off anisotropy for advanced post–collapse evolution of Monte–Carlo models as is seen in  $N$ –body simulations for  $N \leq 2000$ . For simulations with  $N > 10000$  gravothermal oscillations are clearly visible. The calculations of  $N = 2000, 4096, 10000, 32000$  and  $100000$  models take about 2, 6, 20, 130 and 2500 hours, respectively. The Monte–Carlo code is at least  $10^3$  times faster than the  $N$ –body one for  $N = 32768$  with special–purpose hardware (Makino 1996ab). Thus it becomes possible to run several different models to improve statistical quality of the data and run individual models with  $N$  as large as  $100000$ . The Monte–Carlo scheme can be regarded as a method which lies in the middle between direct  $N$ –body and Fokker–Planck models and combines most advantages of both methods.

**Key words:** globular clusters: general — methods: numerical — stars: kinematics

## 1 INTRODUCTION.

Our knowledge about the stellar content, kinematics, and the influence of the environment on observational features of globular clusters and even richer stellar systems are increasing dramatically (Janes 1991, Djorgovski & Meylan 1993, Smith & Brodie 1993, Hut & Makino 1996, Meylan & Heggie 1997). First, observations are reaching the point where segregation of mass within globular clusters can be observed directly and quantitatively. Second, observations have revealed that clusters with dense (collapsed) cores are relatively more concentrated to the galactic center than uncollapsed ones. Thus the influences of the environment and mass spectrum are crucial for cluster evolution. Third, observations give clear evidence that post–collapse globular clusters have bluer cores. This suggests strong influence of dynamical interactions between stars on observational properties of globular clusters. Fourth, recent observations show that many different and fascinating types of binaries and binary remnants are present in abundance in globular clusters. Binaries, in addition to being a diagnostic of the evolution-

ary status of clusters, are directly involved in the physical processes of energy generation, providing the energy source necessary to stop the core collapse and then drive the core expansion. So, to model the evolution of real stellar systems and make meaningful comparison with observation one has to take into account the complex interactions between stellar evolution, stellar dynamics and the environment. Of course all these demands can be fulfilled by direct  $N$ –body codes (but even the  $N$ –body method will have trouble with stellar evolution of binary stars). But they are very time–consuming and they need a special–purpose hardware to be run efficiently (Makino 1996ab). Another possibility is to use a code which is very fast and properly reproduces the standard relaxation process and at the same time provides a clear and unambiguous way of introducing all the physical processes which are important during globular cluster evolution. This task might seem unachievable, but actually this kind of code was in use in the past. Monte–Carlo codes, which use a statistical method of solving the Fokker–Planck equation provide all the necessary flexibility. They were developed by Spitzer (1975, and references therein) and Hénon

(1975, and references therein) in the early seventies, and substantially improved by Marchant & Shapiro (1980, and references therein) and Stodólkiewicz (1986a, and references therein). Unfortunately, lack of fast computers with sufficient memory at that time and development of the direct Fokker–Planck and gaseous models contribute to the abandonment of this method. But recent developments in computer hardware, speed and memory now make it possible to run a Monte–Carlo code efficiently, even on general–purpose workstations. The great advantages of this method, beside of its simplicity and speed, are connected with the inclusion of anisotropy and with the fact that added realism does not slow it down. The Monte–Carlo method can practically cope as easily as the  $N$ –body method with internal freedom of single and binary stars and external environment, with one exception, a stellar system must be spherically symmetric.

The Monte–Carlo code can have another possible use. Despite the simplified nature of continuum models (Fokker–Planck and gaseous models) they will continue for a while to be the most commonly used codes for stellar dynamical evolution. The Monte–Carlo models can be used to optimise physical free parameters and approximations of continuum models to check their validity as it was done in comparison between small  $N$ –body simulations and continuum ones (Giersz & Heggie 1994ab, Giersz & Spurzem 1994). This procedure should further increase our confidence in results obtained by Fokker–Planck or gaseous simulations. On the other hand the Monte–Carlo techniques can be incorporated in continuum models to describe the stochastic processes of binary formation, energy generation and movement (Spurzem & Giersz 1996, Giersz & Spurzem 1997). This, for example, will enable a very detailed investigation of evolution of primordial binaries in evolving background given by an anisotropic gaseous model.

The plan of the paper is as follows. In Section 2 a short review of the ‘old’ and ‘new’ Monte–Carlo methods will be presented. In Section 3 the first results of the ‘new’ Monte–Carlo simulation will be presented. And finally in Section 4 the conclusions and future development of the code will be discussed.

## 2 MONTE–CARLO METHOD.

### 2.1 Basic ideas.

The Monte–Carlo method can be regarded as a statistical way of solving the Fokker–Planck equation. Similarly as the direct Fokker–Planck method it is based on three main assumptions; i.e. **(1)** the gravitational field can be divided on two parts: a smooth, mean field and an irregular, fluctuating field, which causes the cluster evolution, **(2)** the system evolves due to distant two–body interactions through a sequence of essentially steady states, **(3)** the system is spherically symmetric.

The basic idea behind the Monte–Carlo method takes full advantage of these assumptions. During a time interval  $\Delta t$ , much smaller than the relaxation time and larger than the crossing time, the fluctuating gravitational field can be neglected in a first approximation and the system can be regarded as being in a steady state. Because of spherical symmetry of the mean gravitational field the motion of stars is

fully described by simple analytical formulae, an orbit is a plane rosette confined between  $r_{\min}$  and  $r_{\max}$  radii, which are defined (in a given potential) by energy  $E$  and angular momentum  $J$  of a star. However, the fluctuating field causes slow and random changes of the orbit parameters,  $E$  and  $J$ . This effect is small over  $\Delta t$ , but it builds up and becomes significant over the relaxation time scale and it has to be taken into account. To compute it, the influence of all stars in the system at all positions on a test star orbit during the time interval  $\Delta t$  should be considered. It seems that a direct  $N$ –body integration has to be performed to calculate the perturbation. But instead of doing this the standard Monte–Carlo tricks can be applied. The perturbation of a test star orbit is a random quantity, so only its statistical properties matter – the first and second order moments. The exact value of each perturbation is unimportant. The procedure to calculate perturbations is as follows: **(1)** instead of integrating a sequence of uncorrelated small–angle perturbations along the orbit, a single perturbation is computed at a randomly selected point of the orbit, **(2)** instead of considering the effect of all stars in the system, the perturbation is computed locally from a randomly chosen star, **(3)** the computed single perturbation is multiplied by an appropriate factor in order to account for the cumulative effect of all small individual encounters with the rest stars in the system during the past time step. If the procedure is correctly set up, the evolution of the artificial system will be statistically the same as the evolution of the real one.

The way of implementing this basic strategy divides Monte–Carlo codes on three different groups; referred to as ‘Princeton’, ‘Hénon’ and ‘Cornell’ methods (Spitzer 1987, and references therein). Briefly, in the ‘Princeton’ method the stellar orbits are directly integrated with velocity perturbation  $\Delta \mathbf{v}$  chosen to represent proper averages over all types of encounters at each orbital position.  $\Delta \mathbf{v}$  is obtained directly from the standard diffusion coefficients computed for isotropic and Maxwellian velocity distribution of the field stars. The direct integration of the star orbits and computation of velocity changes produced on a single orbit makes it possible to examine violent relaxation and to investigate the rate of escape from an isolated system, respectively. The main disadvantages are that the velocity distributions of test and field stars are different and that the method requires more computing time than other methods.

In the ‘Hénon’ method to compute velocity perturbations produced by encounters the theory of two–body relaxation is used to integrate over the impact parameters of all encounters during the time  $\Delta t$ . Then the main square cumulative value of deflection angle is computed. The effective impact parameter is chosen to give the cumulative deflection angle in a single encounter. A big advantage of this method is that the velocity distributions of the test and field stars are the same and the computing time scales with  $N$  nearly linearly.

In the ‘Cornell’ method the changes of energy  $\Delta E$  and angular momentum  $\Delta J$  resulting from encounters during **integral** number of orbits are computed by use of five orbit–averaged diffusion coefficients:  $\langle \Delta E \rangle_{\text{orb}}$ ,  $\langle \Delta J \rangle_{\text{orb}}$ ,  $\langle \Delta E^2 \rangle_{\text{orb}}$ ,  $\langle \Delta J^2 \rangle_{\text{orb}}$  and  $\langle \Delta E \Delta J \rangle_{\text{orb}}$ . In order to compute these coefficients the velocity distribution of the field stars is equal to suitable isotropized distribution of the test stars. This method is especially suitable for investiga-

tion of physical processes which occur on an orbital time-scale, for example such as: escape of stars or their capture by a central black hole.

Each of these Monte-Carlo implementation was successfully used in simulations of evolution of globular clusters and galactic nuclei. Now I would like to proceed to a more detailed description of Stodólkiewicz's Monte-Carlo scheme, a version of 'Hénon' method, which is the base of the new Monte-Carlo code presented here.

## 2.2 Stodólkiewicz's Monte-Carlo scheme.

The real power of Monte-Carlo codes was demonstrated by Stodólkiewicz (1982, 1985, 1986a). He substantially improved Hénon's version of Monte-Carlo code by adding an individual time-step scheme and a special procedure which very much improves the total energy conservation. His code was used to model the evolution of globular clusters influenced by the following processes: formation of binaries by dynamical and tidal interactions, interaction between binaries and field stars and between binaries themselves, collisions between stars, stellar evolution, the tidal field of the Galaxy and tidal shocks. They were unique calculations and have never been repeated or superseded by anybody.

Because the detailed description of Stodólkiewicz's code was presented more than ten years ago and since then the method was abandoned, I will very briefly describe the basic ingredients of the code. More details can be found in Stodólkiewicz (1982, 1986a).

The evolution of a stellar system is governed by the changes with time of energy (per unit mass)  $E$  and angular momentum (per unit mass)  $J$  of all stars in it. According to the assumptions discussed in the previous section these changes are described by the following equations

$$\frac{dE}{dt} = \frac{\partial U(r, t)}{\partial t} + \left( \frac{dE}{dt} \right)_e, \quad (1)$$

$$\frac{dJ}{dt} = \left( \frac{dJ}{dt} \right)_e, \quad (2)$$

were  $U(r, t)$  is the gravitational potential at distance  $r$  from the cluster center and time  $t$ . The first term on right-hand-side of equation (1) describes the changes of stellar energies caused by the evolution of the gravitational potential, i.e. by changes of the mass distribution – the density in the bulk of system changes slowly while in the core it grows rapidly. The terms with subscript 'e' describe the encounter effects connected with the relaxation process; the driving mechanism of the system evolution.

In the Monte-Carlo method the whole system is divided into  $K$  *superstars* each consisting of a certain number of stars with the same mass  $m$ , distance  $r$  from the cluster center, radial  $v_r$  and tangential  $v_t$  velocities. For each *superstar* changes of  $E$  and  $J$  are computed by the procedures which simulate relaxation processes and changes of gravitational potential. These simulations should give the correct statistical distributions (in practice the mean values) of  $\Delta E$  and  $\Delta J$  for all *superstars*.

The relaxation process of the whole system in the time interval  $\Delta t$  is simulated as a number of single two-body encounters of neighbouring *superstars*, arranged according to their distance from the center. In order to obtain a good

overall effect of the system relaxation over time  $\Delta t$  a very careful approach has to be taken to get the proper effective deflection angle  $\beta$ . This is done in the following way. For a single encounter of two stars with masses  $m_1$  and  $m_2$  and velocities  $\mathbf{v}_1$  and  $\mathbf{v}_2$  the velocity change of the first star is given by

$$m_1(\Delta \mathbf{v}_1)^2 = 4 \frac{m_1 m_2^2}{(m_1 + m_2)^2} w^2 \sin^2 \frac{\beta}{2}, \quad (3)$$

where  $w$  is the relative velocity of interacting stars,  $\beta$  is the angular deflection in the relative orbit of interacting stars. On the other hand the mean overall result of encounters of a test star with the field stars during time  $\Delta t$  is approximately equal to (Hénon 1975)

$$\langle m_1(\Delta \mathbf{v}_1)^2 \rangle = 8\pi G^2 n \Delta t \langle m_1 m_2^2 w^{-1} \rangle \ln(\gamma N), \quad (4)$$

where  $G$  is the gravitational constant,  $n$  is the number density and  $\ln(\gamma N)$  is the Coulomb logarithm. Comparison of equations (3) with (4) leads to the following definition of deflection angle  $\beta$

$$\sin^2 \frac{\beta}{2} = 2\pi G^2 \frac{(m_1 + m_2)^2}{w^3} n \Delta t \ln(\gamma N). \quad (5)$$

Equation (5) connects the relaxation process with the evolutionary time. This is the only equation in which time appears explicitly. The value of  $\beta$  depends on the length of the time-step. The larger time-step the larger  $\beta$ . If the chosen time-step is too large (so that the right-hand-side of equation (5) exceeds unity) the system is underrelaxed and computation depends on the length of the time-step. Therefore, in order to obtain the correct description of the relaxation process, simulations should be conducted with the time-step sufficiently small (smaller than the local relaxation time and larger than the local crossing time) and, as well, dependent on the position in the system (the local relaxation time changes strongly in the system, increasing towards the center). This is done by dividing the whole system on a certain number of zones, for which according to equation (5) the average individual time-steps are computed with  $\beta$  kept in certain boundaries (between 0.025 and 0.05 for equal mass stars). The boundaries for  $\beta$  are chosen experimentally to ensure that the results of simulations are practically independent on the chosen time-step. The zones with the same time-step are collected together forming a larger superzone. The time-steps for successive superzones can only differ by factor of two. The time interval after which the succeeding model of the whole cluster is completed is chosen experimentally and is equal to 0.08 (about one half of the initial half-mass relaxation time). This procedure allows to compute encounters in each part of the system with the time-step several times shorter than the local relaxation time. At the end of the encounter procedure (in the considered superzone) the new velocities for each two interacting stars are computed using the standard scheme (Hénon 1971). This scheme takes into consideration that the plane of relative motion of interacting stars and their relative orbit in this plane can be oriented randomly. This concludes the relaxation step.

Now, the new positions of all *superstars* in the actually computed superzones are chosen. All *superstars* with positive total energy or with distance greater than the tidal radius (for non-isolated system) are treated as escapers. New positions of remaining stars are selected randomly in

their orbits between the pericentre and a maximum distance with the probability proportional to the time, which the star spends in a given place in the orbit. The maximum distance is chosen to be the smallest distance of either apocentre or the position of the last *superstar* in the actually computed superzones. As a result of this procedure, when many successive encounters are included, the  $\Delta E$  and  $\Delta J$  are correctly averaged over the test star orbit. After evaluating the new positions (for all *superstars* in the actually computed superzones) a new distribution of *superstars* has been obtained. This leads to small changes of the mass distribution. The resulting changes of potential with time induce changes in mechanical energy of the *superstars*. This energy change for the  $i$ -th *superstar* in time  $\Delta t$  is given by

$$\Delta E_i = \int \frac{\partial U(r, t)}{\partial t} dt, \quad (6)$$

where the integral is taken along the trajectory of the  $i$ -th *superstar*. Two points of the trajectory are distinguished; the old  $r_{i0}$  and new  $r_{in}$  positions. Both, are chosen randomly in the orbit, which in meantime, changed only slightly due to relaxation process. So they can be treated as representative for the orbit and equation (6) can be approximated by the following expression

$$\Delta E_i = \frac{1}{2}[\Delta U(r_{i0}) + \Delta U(r_{in})], \quad (7)$$

where  $\Delta U = U_n - U_o$  is the difference between the new and old values of the potential in a given point. Comparing equations (6) and (7) and substituting for  $\Delta E_i$  the difference between the new and old total energies of the  $i$ -th *superstar* the new value of velocity  $v_{in}$  is obtained.

$$v_{in}^2 = v_{i0}^2 + U_o(r_{i0}) + U_n(r_{i0}) - U_o(r_{in}) - U_n(r_{in}), \quad (8)$$

where  $v_{i0}$  is the old velocity of the  $i$ -th *superstar* (the old velocity means after relaxation and in old potential). The new tangential velocity  $v_{int}$  is computed using the law of angular momentum conservation. The radial velocity is equal to  $v_{inr} = \sqrt{v_{in}^2 - v_{int}^2}$ . The use of equation (7) to evaluate the new velocities ensures that the total energy of the system practically does not change during the simulations. However, there is an inconsistency in this procedure. New radial velocities are computed at the end of the time-step, while new positions of *superstars* are selected in orbits determined by the old potential. Sometimes this leads to difficulties with determination of new radial velocity. In such situation  $v_{inr}$  is set to zero and the missing energy is subtracted from the energy of next *superstar*. The whole cycle: relaxation process, determination of new positions and determination of new velocities is then repeated for all superzones.

### 2.3 New implementation of Stodólkiewicz's Monte-Carlo method

The Monte-Carlo method briefly described in the previous section is not suitable to correctly represent the very center of the system. In the core, as a result of the collapse, the density in a small and nearly uniform region reaches high values. This area is represented by only a few *superstars*. Therefore the statistical properties of this region are very poorly described. Moreover, *superstars* which belongs to the

core take part in processes which are responsible for energy generation and creation of many different and fascinating types of binaries, binary remnants and coalesced stars in direct stellar interactions. In order to properly describe this region and these processes, in the new code (written from the scratch) each *superstar* is treated as a single star and evolution and motion of all individual objects are followed (this is done not only in the core but throughout the system). This improvement is possible only due to an enormous increase of speed and memory in present day general-purpose computers. Note, that the individual treatment of all objects in the system enables, for example, to investigate the influence of primordial binaries on the system evolution. In Stodólkiewicz's method all binaries or coalesced stars take part only in relaxation process. They were neglected in the computation of the gravitational potential, so the process of mass segregation of binaries and coalesced stars relative to single stars was not properly described.

Stodólkiewicz's procedure to deal with the problems of radial velocity determination after the system adjustment (changes of mechanical energy of the stars due to changes of potential – equations 6–8 above) was slightly changed in the present implementation. If for any star  $v_{in}^2$  is smaller than zero the new radial velocity of a star is set to zero and tangential velocity is computed according to the angular momentum conservation law. The missing kinetic energy is accumulated for all stars which fulfil the above criterion. At the end of relaxation cycle (for the presently computed superzones) the kinetic energy for each star in the system is decreased by a factor equal to the ratio of the total kinetic energy reduced by accumulated missing kinetic energy and the total kinetic energy. This factor is very close to one. If for any star  $v_{inr}^2$  is smaller than zero and  $v_{in}^2$  is bigger than zero the new radial velocity of a star is set to zero and the new tangential velocity is set to  $v_{in}$ . The problem with the determination of the new radial velocity usually occurs when a star is close to the pericentre or apocentre of its orbit. So the assumption that the new radial velocity is equal to zero is well justified. The fraction of 'bad' cases is about 0.01 per cent of all relaxation events. The total accumulated energy of 'bad' cases is only a few percent of the initial total energy of the system.

As it was stated in the previous section the deflection angle  $\beta$  for two interacting stars is chosen to mimic the overall relaxation of these stars with the rest of the system over the time  $\Delta t$ . Then  $\beta$  is the accumulated deflection angle and it is usually bigger than the deflection angle for an individual small-angle interaction. This can lead to an overestimation of the number of stars which escape from the system (particularly for stars on very elongated orbits with binding energy very close to zero). Indeed, preliminary, test Monte-Carlo simulations showed too high an escape rate comparable to direct  $N$ -body results. It is worth to note that the Stodólkiewicz's Monte-Carlo code (Stodólkiewicz 1982) also gave a too high escape rate compared to results of  $N$ -body simulations available at that time. Hénon (1961) pointed out that the escape process is not a diffusive one, but has to be regarded as a two-body interaction which directly leads to escape of a star. This point was further modified by Spitzer & Shapiro (1972), who pointed out that the distribution function of stars itself evolves on a relaxation time-scale, and then a star that has diffused to energies a little below

the escape limit can escape in a single two-body encounter in the core. Giersz & Heggie (1984a) further modified this point showing that anisotropy has a large effect on the escape rate. The larger anisotropy the larger escape rate. So to properly describe the escape process in the Monte-Carlo code (according to the discussion above) the following procedure was introduced **only** for stars which escape due to standard relaxation process. The probability that the closest encounter has impact parameter less than  $p$  in time  $\Delta t$  is given by

$$F(x) = 1 - e^{-\lambda x} \quad (9)$$

where  $x = \pi p^2$  is the area of a disc with radius  $p$  and  $\lambda = nw\Delta t$  is the number of interactions per unit area. So the resulting distribution function (probability density) of impact parameters is as follows

$$f_p(p) = \left(\frac{dF}{dx}\right) \left(\frac{dx}{dp}\right) = 2\pi nwp\Delta te^{-\pi nwp\Delta tp^2} \quad (10)$$

Using the values of  $n$  and  $w$  from the computation of the relaxation process (for two considered stars), a new impact parameter is picked up randomly according to equation (10). The deflection angle is connected with the impact parameter by the following formula

$$\sin^2 \frac{\beta}{2} = \frac{1}{\left(1 + \left(\frac{p}{p_o}\right)^2\right)} \quad (11)$$

where  $p_o = G(m_1 + m_2)/w^2$  is the impact parameter for the  $90^\circ$  deflection angle. So using again equation (3) and the scheme described by Hénon (1971) the new velocities of two interacting stars can be found. If one of the two stars has positive binding energy it is regarded as a escaper and second star is kept in the system with the new velocity, otherwise two stars are kept in the system with the newly obtained velocity. If no star would escape in the normal Monte-Carlo step, then it would not escape in the new procedure (the new procedure is only invoked if escape occurs in the usual procedure). In principle, therefore, the new procedure underestimates the escape. However, the underestimate should be small, because it will almost always be true that the right-hand-side of equation (11) is much smaller than that of equation (5). The results of Monte-Carlo simulations presented in the next section strongly suggest that the procedure discussed above represents in a proper way physics behind the escape process. Nevertheless, other explanations of the too high escape rate in Monte-Carlo simulations comparable to  $N$ -body simulations are possible. For example, small deviations from spherical symmetry of the system can cause small changes of angular momenta of the stars on very elongated orbits (Rauch and Tremaine 1996) leading to fewer escapers in  $N$ -body simulations. However, this process can not be investigated by the Monte-Carlo code.

Basically, the improvements mentioned above are the only major changes to Stodólkiewicz's original code. Other changes are rather cosmetic and do not have any influence on the code flow or implementation of any physical processes. However, before proceeding further I will briefly describe how binaries are introduced to the code (in the case

of single-mass system – the case of multi-mass system will be discussed in the next paper).

As it was mentioned at the beginning of this section all stellar objects, including binaries, are treated (in the new code) as single *superstars*. This allows, in a simple and accurate way, to introduce to the code the processes of stochastic formation of binaries and their subsequent stochastic interaction with field stars and other binaries. The whole procedure is introduced in a few separate steps. First of all a new binary has to be formed. The standard formula for the rate of three-body binary formation (Hut 1985) gives the probability of binary formation as

$$P_{3b} = \int \int 0.9G^5 m^5 n^3 \sigma^{-9} dV dt, \quad (12)$$

where  $m$  is the mass of single stars and  $\sigma$  is the one-dimensional local velocity dispersion. The integration is over volume and time. The probability of binary formation is computed for each time step and for each zone containing three successive *superstars*, starting from the zone closest to the system center. The computed probability is compared with a random number drawn from the uniform distribution. If the probability is smaller than the random number a binary is formed from the first and second star in the zone, at the position of the center of mass of these two stars. The procedure is repeated for all (three-stars) zones in the system. For the binding energy of the newly formed binary the value of  $3kT$  is adopted, which is usually used as a minimum binding energy of permanent binaries (Hut 1985). Before reaching this threshold energy the binary has been living for some time in the cluster and interacting with field stars. Assuming that its centre of mass is in energy equipartition with field stars, the orbit of the new binary in the cluster can be computed.

A binary living in the cluster is influenced by close and wide interactions. Wide interactions only change its movement in the system (relaxation process) and close interactions change also its binding energy. To simulate close interactions the procedure suggested by Stodólkiewicz (1986a) was adopted. First, the check is performed, whether a close interaction is due. The probability of binary field star interaction is computed using Spitzer's formula (Spitzer 1987). This probability is as follows

$$P_{3b*} = \int \int \frac{5\pi A_S G^2 m^3 n}{6\sigma E_b} dV dt, \quad (13)$$

where  $E_b$  is the binary binding energy and  $A_S$  is a coefficient equal to 21. The integration is over volume and time. This probability is computed for each binary and compared with a random number drawn from the uniform distribution. If the binary is due to interaction with a field star the change of its binding energy is computed according to the distribution function of energy changes (Spitzer 1987),  $f(z) = \cos^6 z$ , where  $z = \arctan(\Delta E_B/E_B)$ . The energy,  $\Delta E_B$ , generated in the interaction is distributed between the single star ( $2\Delta E_B/3$ ) and the binary centre of mass ( $\Delta E_B/3$ ). Knowing the orbit of the binary, we know its radial and tangential velocities at any point in the orbit. The absolute value of the recoil velocity of the binary  $\Delta v$  is determined from the quadratic equation

$$\Delta v^2 + 2(v_r \cos \theta + v_t \sin \theta \cos \phi)\Delta v - \frac{2\Delta E_b}{m_b} = 0, \quad (14)$$

where  $v_r$  and  $v_t$  are the initial radial and tangential velocities of the binary centre of mass, respectively,  $\theta$  and  $\phi$  are the randomly chosen direction of the recoil determined according to the distribution  $f(\theta) = \sin \theta/2$  for  $\theta \in (0, \pi]$  and uniform distribution for  $\phi \in (0, \pi]$ , respectively.  $m_b$  is the binary mass. The new components of the binary centre of mass velocity are directly computed from the old velocities,  $\Delta v^2$  and chosen  $\theta$  and  $\phi$ . Having new velocities the new orbit of the binary is determined. The same procedure is adopted for the determination of the new orbit and the new radial and tangential velocities of the single star which just interacted with the binary.

Now the first, pilot results of the evolution of isolated single mass systems conducted by the new code will be presented.

### 3 FIRST RESULTS

The Monte–Carlo code contains several free parameters, which have to be adjusted in order to get the proper representation of the system evolution. The most important parameters are: the boundaries for the deflection angle  $\beta$ , the number of stars used to estimate the local density, the time interval after which the succeeding models of the whole system are computed, the coefficient in the Coulomb logarithm and scattering cross–section for interaction between binaries and field stars. Note: except the last two parameters, they are not physical but technical, mainly used to facilitate simulations. The best way of adjusting them is to compare the new results of Monte–Carlo simulations with direct  $N$ –body data. The same strategy was used to optimise the free physical parameters of the continuum models (Giersz & Heggie 1994ab, Giersz & Spurzem 1994).

High quality statistical data for single–mass  $N$ –body simulations are available only for  $N = 250, 500, 1000, 2000, 4096$  and  $10000$  (Giersz & Heggie 1994ab, Giersz & Spurzem 1994, Spurzem & Aarseth 1996). The simulations with  $N = 250$  and  $500$  should be excluded from the comparison, because strong two–body encounters have too much influence on the dynamical evolution of these systems (Giersz & Heggie 1994ab, Giersz & Spurzem 1994). This is in contradiction to one of the main assumption on which the Monte–Carlo method is based. Models with  $N = 1000$  are extended only up to one collapse time after the core bounce. This is too small to properly compare the long–term post–collapse evolution. The same situation is for model  $N = 10000$  which is extended just over the time of core bounce. Simulations with  $N = 2000$  and  $4096$  are the best for our purposes. They cover evolution up to twelve collapses time and consist of several separate runs (for  $N = 2000$ ). Additionally, because of a good statistical quality of the data, model with  $N = 10000$  was used to compare the core collapse and core bounce phases of the evolution. Only results for  $N = 2000$  were averaged over 25 simulations, each having the same initial parameters but with a different sequence of random numbers used to initialise the positions and velocities of the stars (Giersz & Heggie 1994a). For other  $N$  only individual simulations were used to compare with  $N$ –body runs.

For all simulations (of isolated single–mass systems of point mass particles) presented in this paper the Plummer model was used as the initial condition. The standard  $N$ –

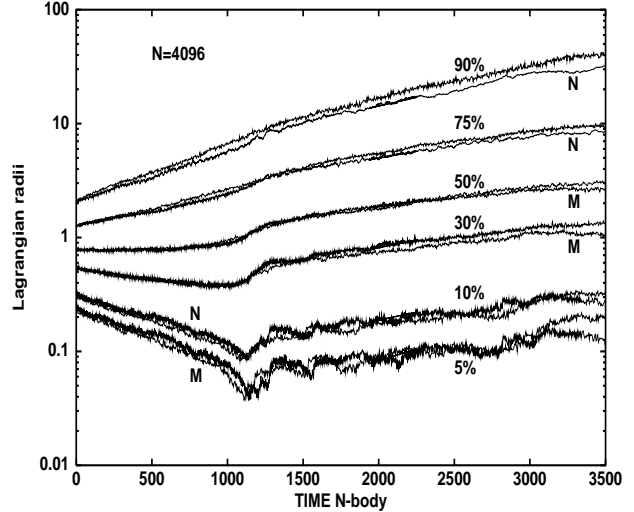


**Figure 1.** Evolution of Lagrangian radii for  $N = 4096$  for Monte–Carlo model (M) and  $N$ –body model (N).

body units (Heggie & Mathieu 1986); total mass  $M = 1$ ,  $G = 1$  and initial energy equal to  $-1/4$  have been adopted for all runs. Monte–Carlo time means the  $N$ –body time divided by  $N/\ln(\gamma N)$ .

Very extensive and time consuming calculations were performed to adjust the free parameters of the Monte–Carlo code. It should not be surprised that the best choice of the free parameters is similar to that chosen by Stodólkiewicz (1982). The boundaries for  $\beta$  are 0.025 and 0.05 (0.0125 and 0.025 for large  $N$ ). The time interval, between consecutive, complete models, is about 0.0075 – 0.01 (about one twentieth of the initial half–mass relaxation time). A lot of care was taken to properly estimate the local density, which play an important role in determination: the deflection angle, the number of created three–body binaries and the number of interactions between binaries and field stars. Again, the number of star chosen to determine it was similar to that used by Stodólkiewicz (1982). Results presented by Giersz & Heggie (1994ab) suggest that value of  $\gamma = 0.11$  for the coefficient in the Coulomb logarithm and the scattering cross–section given by Spitzer (1987) assure the best agreement with  $N$ –body data. Therefore these parameters were used in Monte–Carlo simulations presented in this paper.

Generally, for both models (Monte Carlo and  $N$ –body) the phase of core collapse is remarkably similar (Figure 1 for  $N = 4096$ ). For  $N = 2000$  (not shown here – see Giersz 1996), the first differences start to build up around the time of core bounce. This is particularly well visible for middle and outer Lagrangian radii. The rate of system expansion in the  $N$ –body models is slightly faster than in the Monte–Carlo models. This behaviour is even more pronounced for the anisotropy distribution (not shown here – see Giersz 1996). In the advanced phase of core expansion there is no level off anisotropy, feature which is so characteristic for  $N$ –body simulations with  $N \leq 2000$  (Giersz & Heggie 1994b and Giersz & Spurzem 1994). Probably, for simulations with small  $N$  the relaxation process is slightly overestimated. Encounters between stars are stronger and more stars are

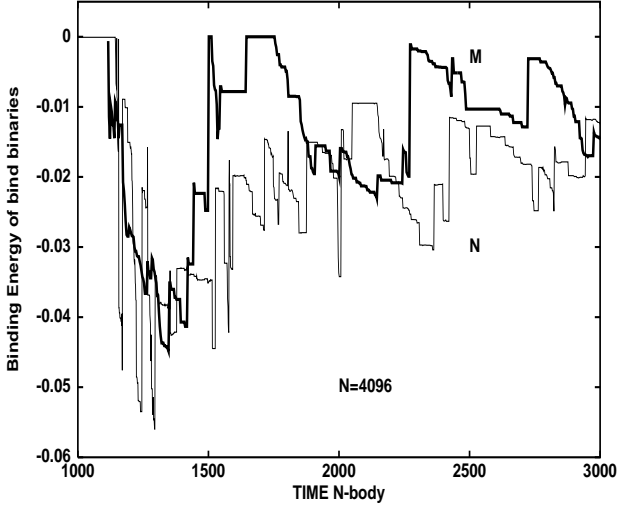


**Figure 2.** The binding energy of binaries bound to the system for  $N = 4096$  for Monte-Carlo model (M – thick line) and  $N$ -body model (N).

put on elongated orbits what leads to bigger anisotropy and faster expansion rate. It seems that this behaviour of Monte-Carlo simulations (for small  $N$ ) can not be cured by an appropriate selection of the free parameters. For  $N = 4096$  in the first phase of the core expansion the agreement between both models is very good (see Figure 1) but later on the disagreement starts to build up. Outer parts of the Monte-Carlo models expand too fast comparably to  $N$ -body models. And even the inner Lagrangian radii (except 5 and 10 per cent Lagrangian radii) show disagreement (Monte-Carlo models evolve too fast), but at least this can be partially associated with the individual statistical ‘noise’ of simulations. Different amounts of energy generated by binaries and different times at which energy generation take place can lead to substantial differences between simulations for advance post-collapse evolution.

It is worth to note that the collapse time for Monte-Carlo and  $N$ -body models is practically the same (taking into account the statistical spread between simulation with the same  $N$ ). This further confirms the value of  $\gamma = 0.11$ , in the Coulomb logarithm, obtained by comparison of small  $N$ -body and continuum models (Giersz & Heggie 1994a).

The energy conserved during the simulations can be divided on the following parts: total external energy of the system (sum of the total kinetic and potential energies), total energy of star escapers, total energy of binary escapers, total internal binding energy of binary escapers and total internal binding energy of bound binaries. Figure 2 shows for both models ( $N = 4096$ ) the binding energy of binaries bound to the system. The agreement between the models is very good (taking into account the statistical ‘noise’). Even the size and amplitude of the energy bump around the time of core collapse is very similar. This guarantees that for both models around the time of core bounce the expansion rate and the shape of the inner Lagrangian radii curves are nearly the same. Later on, however, the total binding energy of bound binaries is systematically smaller than in the  $N$ -

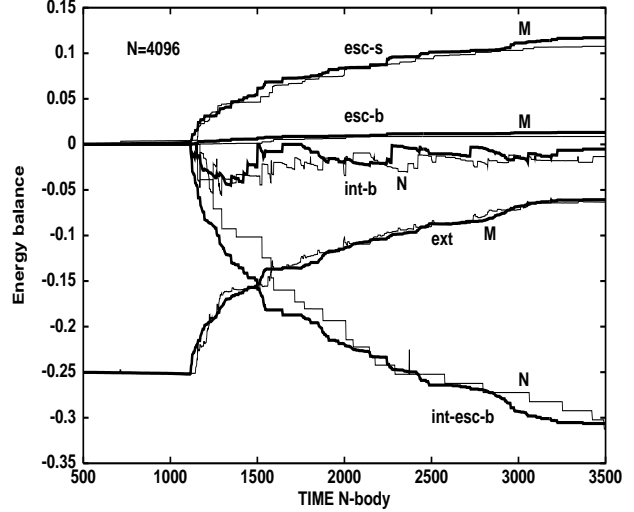


**Figure 3.** Energy balance for  $N = 4096$  for Monte-Carlo model (M – thick line) and  $N$ -body model (N). Esc-s - total energy of star escapers, esc-b - total energy of binary escapers, int-b - total binding energy of bound binaries, int-esc-b - total binding energy of escaped binaries, ext - external energy of the system.

body simulations. Correspondingly the total binding energy of escaped binaries is bigger for Monte-Carlo models to balance the differences for binding energies of bound binaries. The external binding energy of the system and escape energies of single and binary stars are remarkably similar (see Figure 3). For  $N = 2000$  agreement between models is not so good (see Giersz 1996). Around the time of core bounce the bump in the total binding energy of bound binaries is smaller and more shallower for Monte-Carlo models than for  $N$ -body ones. So the resulting expansion of the middle and outer parts of the system is less abrupt for Monte-Carlo simulations. Also energy of escapers and total binding energy of escaped binaries is bigger for Monte-Carlo models during advanced post-collapse evolution. This at least partially leads to higher anisotropy and expansion rate for Monte-Carlo models for middle and outer Lagrangian radii.

The example of an anisotropy evolution for Monte-Carlo simulations ( $N = 32000$ ) is presented on Figure 4. Anisotropy is defined as  $A = 2 - V_t^2/V_r^2$ , where  $V_t$  and  $V_r$  are the tangential and radial velocity dispersions, respectively. Each was computed as a mass-weighted average taken over all stars within shells bounded by consecutive Lagrangian radii. There is no discernible anisotropy in the innermost shells, up to the Lagrangian radius 10 per cent of the mass. For intermediate and outermost shells anisotropy starts to increase from the very beginning, the faster the further from the centre of the system. For intermediate shells, at the time of core bounce (when the binaries start to influence the core evolution) sharp increases of anisotropy can be seen. Then the rate of increase of anisotropy slows down, but there is no level off anisotropy (Giersz & Heggie 1994b). Finally, for the outermost shells, shortly after the core bounce, anisotropy reaches a maximum value, which is very close to 2. The outermost parts of the system are practically populated by stars on radial orbits.

In Figure 5 the number of escapers for  $N = 4096$  for

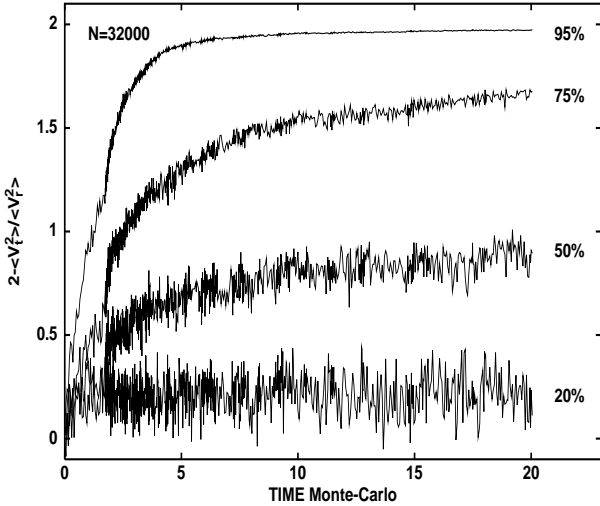


**Figure 4.** Evolution of the anisotropy averaged within mass shells defined by the Lagrangian radii (15-20, 45-50, 70-75, 90-95 per cent) as a function of time for  $N = 32000$  for Monte-Carlo simulations.

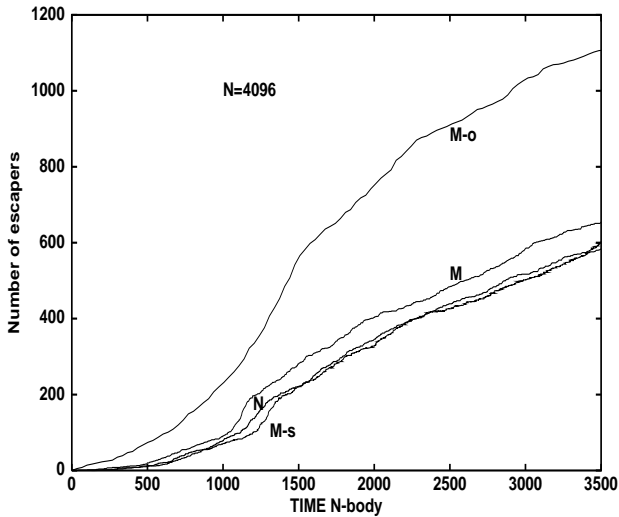


**Figure 5.** Number of escapers for  $N = 4096$  for  $N$ -body model (N) and Monte-Carlo models: with better treatment of escapers (M), without that treatment (M-o) and with shifted data (M-s) - see the text for more explanations

$N$ -body simulations and Monte-Carlo simulations with different treatment of escapers (see previous section) is shown. Only because of a better treatment of escaped stars (described in the previous section) the agreement between both curves (labelled by  $N$  and  $M$ ) is reasonably good. Without this procedure differences would be roughly 80 per cent (curve labelled by  $M$ -o). For  $N$ -body simulations there is a delay in removing escaped stars from the system (stars have to travel distance up to ten times the half-mass radius – for Monte-Carlo simulations are removed instantaneously). To account for that the Monte-Carlo curve in Figure 5 was shifted in time by  $150r_h/r_{ho}$   $N$ -body time units (in  $N$ -body

model the first star escapes at time 155). The ratio of present to initial half-mass radii takes in a very simplifying way into account the fact that in the course of evolution the system expands and more time is needed for stars to escape. The both curves (labelled by  $N$  and  $M$ -s on Figure 5) come to very close agreement. This confirms the simple idea about time-dependent shift and source of disagreement between curves  $M$  and  $N$  in Figure 5. It is worth to note that the escape rate for Monte-Carlo simulations (with 'special' treatment of escapers) for  $N = 2000$  and  $N = 10000$  is also in good agreement with  $N$ -body simulations.

Comparison between the Monte-Carlo simulations and the  $N$ -body ones for  $N = 10000$  shows, basically, the same features as in the case of  $N = 4096$ .

Gravothermal oscillations are the most pronounced feature of the post-collapse evolution of  $N$ -body systems with a number of stars greater than a few thousands. They were observed in gas (Bettwieser & Sugimoto 1984, Goodman 1987, Heggie & Ramamani 1989, Spurzem 1994), Fokker-Planck (Cohn et al 1986, Cohn, Hut & Wise 1989, Gao et al 1991, Takahashi & Inagaki 1991) and recently in  $N$ -body simulations (Makino 1996ab). The lowest value of  $N$  for which gravothermal oscillations begin to show up is uncertain. For continuum models it is around 7000. A pilot  $N$ -body simulation of system consisting of 16384 particles (Makino 1996ab) shows clear oscillations. There are also some signs of gravothermal oscillations in  $N$ -body simulations for 5000 particles (Heggie 1995) and even smaller  $N$  (Makino, Tanekusa & Sugimoto 1986, Makino 1989). All these results suggest that gravothermal oscillations should be as well present in Monte-Carlo simulations (discussed here), at least for  $N = 32000$  or more. It is worth to note that in unpublished Monte-Carlo simulations for  $N = 100000$  conducted by Stodórkiewicz (1986b) there are some signs of gravothermal oscillations (see Giersz 1996). In Figure 6 the evolution of the logarithm of the central density is presented for  $N = 4096$ , 10000, 32000 and 100000, respectively. For  $N = 4096$  there are some oscillation features, but they are practically undistinguishable from fluctuations. For  $N = 10000$  oscillations are more visible (for example around the time 3 or 12), but still it is difficult to judge if they are clearly gravothermal. However, for larger values of  $N$  there is no doubt that the gravothermal oscillations are present, as will be proven in more details below. It should be noted that for oscillations observed in Monte-Carlo simulations there is no clear transition from regular oscillations to chaotic ones or from stable expansion to oscillations. Features observed in gas and Fokker-Planck models (Heggie & Ramamani 1989, Breeden et al 1994). However, the present results are consistent with results obtained by Takahashi & Inagaki (1991) for stochastic Fokker-Planck model (stochastic binary formation and energy generation), by Makino (1996ab) for  $N$ -body simulations and by Giersz & Spurzem (1997) for anisotropic gaseous model with fully self-consistent Monte-Carlo treatment of binary population. This further supports the suggestion given by Takahashi & Inagaki (1989) that for stochastic systems gravothermal oscillations are more chaotic and unstable.

Now, let's take a closer look on run with  $N = 100000$  particles and examine in more details the phases of expansions. It is widely accepted that a long expansion phase without significant energy generation and with temperature



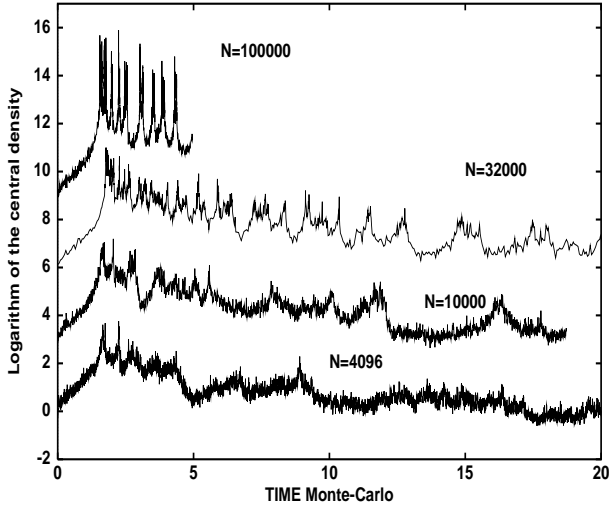


**Figure 6.** Evolution of the central density for  $N = 4096$ , 10000, 32000 and 100000. Data are shifted in the logarithm by 3, 6 and 9 for  $N = 10000$ , 32000 and 100000, respectively.

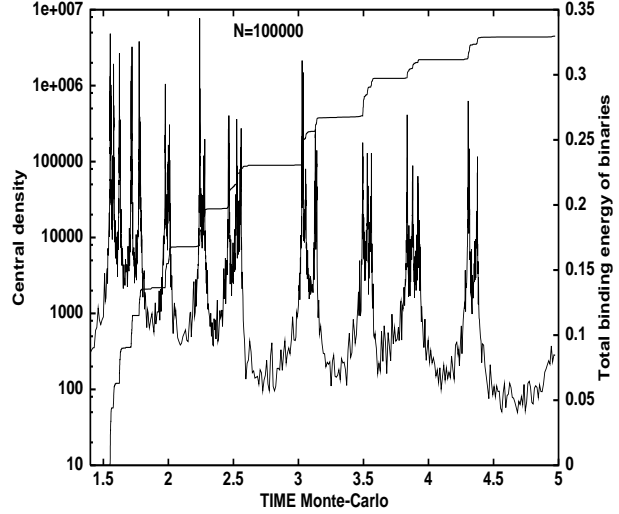


**Figure 8.** Evolution of the central density and the total binding energy of binaries (stepped curve) for  $N = 100000$ .

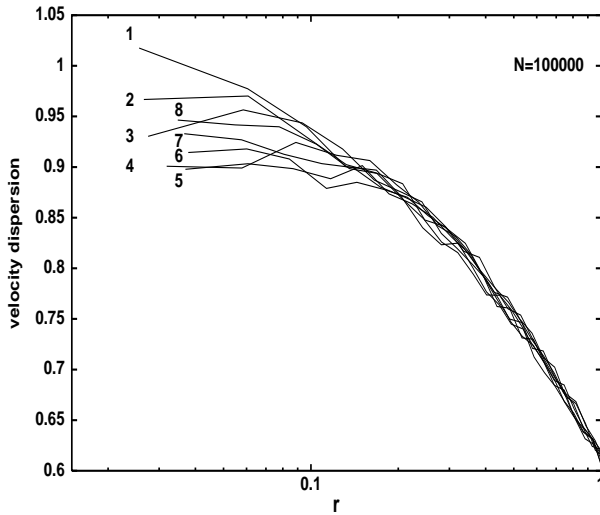


**Figure 7.** Velocity distribution for  $N = 100000$  for a sequence of time outputs during the expansion phase around time 2.5 (see Figure 8). Labels from 1 to 8 are for increasing time.

inversion (during this phase) are the most important signatures of gravothermal expansion (Bettwieser & Sugimoto 1984, McMillan & Engle 1996). In Figure 7 the velocity distribution is presented for a sequence of time outputs during the huge oscillation around the time 2.5 (see Figure 8). Despite the fact that the velocity distribution is plotted every 2 per cent Lagrangian radii the temperature inversion is very clearly visible for curves labelled 2, 3 and 4 (see Figure 7). The temperature inversion is bigger than 4 per cent (taking into account that the central temperature is slightly smaller than temperature at the 2 per cent Lagrangian radius). This value is in a very good agreement with results of gas (Bettwieser & Sugimoto 1984, Heggie

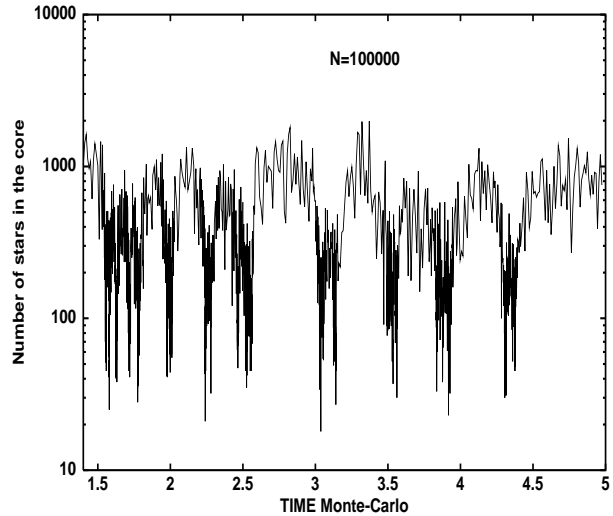


**Figure 9.** Evolution of the number of particles in the core for  $N = 100000$ .

& Ramamani 1989), Fokker-Planck (Cohn et al. 1989) and  $N$ -body (Makino 1996ab) models. Now lets concentrate on the phases of energy generation. Figure 8 shows an enlarged view of the time variation of the central density and the total binding energy of binaries. It is clear that energy is mostly generated when system is found in maximum density phases and expansion is mainly driven without binary energy generation. There are visible several such expansions. All these expansions continue much more than hundreds of the central relaxation times. For expansions driven by binaries it could not continue for more than one hundred central relaxation time (Makino 1996b). Two expansion phases are exceptional (around the time 2.5 and 4.3). Their duration is much longer than for any other oscillation. There is no obvious other explanation for that than gravothermal os-

oscillations. Indeed, results of anisotropic gaseous simulations for  $N = 100000$  conducted by Spurzem (1994) show that oscillations presented in  $\zeta$ ,  $\log(\rho_c)$  and  $\log(v_c)$  space (where  $\zeta = t_{rc} \mathrm{d} \ln(\rho_c) / \mathrm{d} t$ ,  $\rho_c$ ,  $v_c$  and  $t_{rc}$  are the central density, velocity dispersion and relaxation time, respectively) form an attractor, which is characterised by two large and several very small loops. For both models (gaseous and Monte-Carlo) the attractors projected on  $v_c$  plane are remarkably similar in the range of central density,  $\zeta$  and as well in the shape and size of large loops. This suggests that despite the strong stochasticity of  $N$ -body systems the underlying physics of gravothermal oscillations for continuum models is at least partially fulfilled. It is worth to note that there are visible several short period and low amplitude oscillations on Figure 8. These oscillations are probably connected with stronger binary activities (significant energy generation) and they are not mainly driven by the temperature inversion the core. So, the picture that only part of oscillations are truly gravothermal (McMillan & Engle 1996) is further supported by the Monte-Carlo simulations. In Figure 9 is shown the evolution of number of particles in the core for  $N = 100000$ . The number of particles at the phases of maximum contraction is around 20, while for the phases of maximum expansion is around 1000. This result is in excellent agreement with  $N$ -body calculations (Makino 1996ab) and as well with gas and Fokker-Planck calculations (Heggie & Ramamani 1989, Breeden et al 1994). This further strengthens the fact that gravothermal oscillations observed in the Monte-Carlo simulations are practically undistinguished from that for direct  $N$ -body simulations.

From the data shown it is concluded that oscillations are indeed present in Monte-Carlo simulations with  $N \geq 32000$  particles and possible with  $N = 10000$  particles. This is the first unambiguous detection (Giersz 1996) of gravothermal oscillations in Monte-Carlo simulations. This finally closed the list of methods used to investigate evolution of large collisional systems for which theoretical prediction of gravothermal oscillations was confirmed.

Finally, a few words about the efficiency of the new code. The calculations of  $N = 2000$ , 4096, 10000 and 32000 and 1000000 models were conducted on PC-Pentium 166MHz and took about 2, 6, 20, 130 and 2500 hours, respectively. Taking into account the fact that  $N$ -body simulations for  $N = 32768$ , up to the core bounce, performed by Makino (1996ab) took 3 months on 1/4 GRAPE-4 (Teraflop special-purpose hardware) it can be easily shown that Monte-Carlo simulations are at least  $10^5$  times faster than  $N$ -body ones. The theory for Monte-Carlo models predicts a linear increase of computing time with  $N$ . This is connected with the fact that the potential computation is the most time consuming part of the code. In the Monte-Carlo model due to spherical symmetry of the system the potential computation is proportional to  $N$ . However the real calculations show a steeper dependence on  $N$  than theory predicts. It seems that this is connected with the fact that larger systems spend more time in phases of high central density (gravothermal oscillations). They have more density peaks, which imply smaller time steps in order to properly resolve their evolution.

The high speed of the new Monte-Carlo code makes possible to run several different models with modest  $N$  to improve statistical quality of the data and run individual

models with  $N$  as large as 100000. This is a first step in a direction to simulate real large  $N$ -body systems.

#### 4 CONCLUSIONS AND FUTURE DEVELOPMENTS OF THE NEW MONTE-CARLO CODE

A successful revision of Stodółkiewicz's Monte-Carlo code was presented. The updated method treats each *superstar* as a single star and follows the evolution and motion of all individual stellar objects. This improvement was possible thanks to the recent developments in computer hardware and computer speed. Two essential changes were added to the original Monte-Carlo code. Firstly, the procedure which deal with problems of radial velocity determination after the system rearrangement (changes of mechanical energy of the stars due to changes of mass distribution) was slightly changed. This assures better energy conservation. Secondly, the new procedure which deals with star escapers was added. This practically resolves the problem with too high escape rate observed in Monte-Carlo simulations. The Monte-Carlo scheme presented here (as previous Monte-Carlo schemes) takes full advantage of the undisputed physical knowledge on the secular evolution of (spherical) star clusters as inferred from continuum model simulations. Additionally it describes in a proper way the graininess of the gravitational field and the stochasticity of the real  $N$ -body systems. This does not include any additional physical approximations or assumptions which are common in Fokker-Planck and gas models (e.g. conductivity or isotropic distribution function for field stars). From that respect Monte-Carlo scheme can be regarded as a method which lies in the middle between direct  $N$ -body and Fokker-Planck models and combines most advantages of the both methods.

The first calculations for equal-mass  $N$ -body systems with three-body energy generation according to Spitzer's formulae show good agreement with direct  $N$ -body calculations for  $N = 2000$ , 4096 and 10000 particles. The density, velocity, mass distributions, energy generation, number of binaries etc. follow the  $N$ -body results. Only the number of escapers is slightly too high compared to  $N$ -body results (but this can be resolved by the time-dependent shift of the escape rate) and there is no level off anisotropy for advanced post-collapse evolution of Monte-Carlo models as is seen in  $N$ -body simulations for  $N \leq 2000$ . For simulations with  $N > 10000$  gravothermal oscillations are clearly visible. This is the first unambiguous detection of gravothermal oscillations in Monte-Carlo simulations. Moreover, this is a first unambiguous detection of gravothermal oscillations for stochastic  $N$ -body system with  $N$  as large as 100000.

The speed of the new code makes it possible to run individual models with  $N$  as large as 100000 and also enables, in an unambiguous way, the inclusion of several different physical processes which operate during different stages of evolution of real globular clusters.

The new Monte-Carlo code described in this paper is seen as a first step towards realistic models of globular clusters. Several important physical processes have to be included to make the simulations of the stellar systems more realistic. The final code will contain the following physical processes: (1) formation of binaries due to dynamical and

tidal interactions, (2) primordial binaries, (3) stellar evolution, (4) tidal field of Galaxy and tidal shocks connected with crossing the galactic plane and with large molecular clouds, (5) collisions between stars, (6) interactions between binaries and stars and between binaries themselves, improving the presently used scattering cross-sections for binary hardening.

In the first stage all processes connected with interactions between objects were modelled using analytical cross sections available in the literature. This allowed the code to be tested, and made possible comparison with continuum models.

In the next stage interactions between groups of three and four stars will be modelled by numerical integrations of their orbits (the first attempts are tested now). If during the integration the distance between two or more stars becomes smaller than the sum of their radii then a physical collision takes place. This more realistic approach ensures that processes of energy generation (the most important factor in the dynamical evolution of globular clusters) will be modelled more closely.

The final stage will be the inclusion of detailed 3-D hydrodynamical modelling of collisions between stars. This will be done by use of Smooth Particle Hydrodynamics (SPH) for a limited number of particles per star (a few hundred). This will allow close comparison between numerical models and observations of real globular clusters. I refer here to observations of various, peculiar objects like blue stragglers and milliseconds pulsars, which can be formed during collisions and encounters between stars.

**Acknowledgments** I would like to thank Douglas C. Heggie and Rainer Spurzem for stimulating discussions, comments and suggestions to a draft version of this paper. I also thank Douglas C. Heggie, who made the  $N$ -body results for  $N = 4096$  particles available. This work was supported in part by the Polish National Committee for Scientific Research under grant 2-P304-009-06.

## REFERENCES

- Bettwieser E. & Sugimoto D., 1984, MNRAS, 208, 498  
 Breeden J.L., Cohn H.N. & Hut P., 1994, ApJ, 421, 195  
 Cohn H., Hut P., 1989, ApJ, 226, 1087  
 Cohn H., Wise M.W., Yoon T.S., Statler T.S., Ostriker J., Hut P., 1986, in Hut P., McMillan S., eds., The Use of Supercomputers in Stellar Dynamics, New York: Springer, 206  
 Djorgovski S.G. & Meylan G., eds., 1993, Structure and Dynamics of Globular Clusters. A.S.P., San Francisco  
 Gao B., Goodman J., Murphy B., Cohn H., 1991, ApJ, 370, 567  
 Giersz M., 1996, in IAU Symp. 174, Dynamical Evolution of Star Clusters, ed. P.Hut & J. Makino(Boston:Kluwer),101  
 Giersz M. & Heggie D.C., 1994a, MNRAS, 268, 257  
 Giersz M. & Heggie D.C., 1994b, MNRAS, 270, 298  
 Giersz M. & Spurzem R., 1994, MNRAS, 269, 241  
 Giersz M. & Spurzem R., 1997, in preparation  
 Goodman J., 1987, ApJ, 313, 576  
 Heggie D.C., 1995, private communication  
 Heggie D.C. & Mathieu R.M., 1986, in Hut P., McMillan S.L.W., eds., The Use of Supercomputers in Stellar Dynamics., Springer Berlin, 233  
 Heggie D.C., & Ramamani N., 1989, MNRAS, 237, 757  
 Hénon M., 1961, Ann. Astrophys., 24, 369  
 Hénon M., 1971, Astrophys. Sp. Sci., 14, 151  
 Hénon M., 1975, in Hayli A., ed., Dynamics of Stellar Systems, Reidel: Dordrecht, 133  
 Hut P., 1985, in Goodman J., Hut P., eds, Proc. IAU Symp. 113, Dynamics of Star Clusters, Reidel, Dordrecht, p. 231  
 Hut P. & Makino J., eds. 1996, Dynamical Evolution of Star Clusters. A.S.P., San Francisco  
 Janes K., ed. 1991, The Formation and Evolution of Star Clusters. A.S.P., San Francisco  
 Makino J., 1989, in Dynamics of Dense Stellar Systems, ed. D. Merritt (Cambridge: Cambridge Univ. Press), 201  
 Makino J., 1996a, in IAU Symp. 174, Dynamical Evolution of Star Clusters, ed. P. Hut & J. Makino (Boston:Kluwer), 141  
 Makino J., 1996b ApJ, 471, 796  
 Makino J., Tanekusa J. & Sugimoto D., 1986, PASJ, 38, 865  
 Marchant A.B. & Shapiro S.L., 1980, ApJ, 239, 685  
 McMillan S.L.W. & Engle E.A., 1996, in IAU Symp. 174, Dynamical Evolution of Star Clusters, ed. P. Hut & J. Makino (Boston:Kluwer), 379  
 Meylan G., & Heggie D.C., 1997 in The Astronomy and Astrophysics Review, in press  
 Rauch K.P., & Tremaine S., 1996, New Astronomy, 1, 149  
 Smith G.H & Brodie J.P, eds., 1993 The Globular Cluster-Galaxy Connection. A.S.P, San Francisco  
 Spitzer L., Jr., 1975, in Hayli A., ed, Dynamics of Stellar Systems, Reidel: Dordrecht, p.3  
 Spitzer L., Jr., 1987, Dynamical Evolution of Globular Clusters. Princeton Univ. Press, Princeton, 77  
 Spitzer L., Jr. & Shapiro S.L., 1972, ApJ, 173, 529  
 Spurzem R., 1994, in Ergodic Concepts in Stellar Dynamics, eds. D. Pfenniger & V.G. Gurzadyan (Springer-Vlg., Berlin, Heidelberg), 170  
 Spurzem R. & Aarseth S.J., 1996, MNRAS, 282, 19  
 Spurzem R. & Giersz M., 1996, MNRAS, 283, 805  
 Stodólkiewicz J.S., 1982, Acta Astr., 32, 63  
 Stodólkiewicz J.S., 1985, in Goodman J. & Hut P., eds., Dynamics of Star Clusters, Reidel:Dordrecht, 361  
 Stodólkiewicz J.S., 1986a, Acta Astr., 36, 19  
 Stodólkiewicz J.S., 1986b, private communication  
 Takahashi K. & Inagaki S., 1991, PASJ, 47, 561

This paper has been produced using the Royal Astronomical Society/Blackwell Science L<sup>A</sup>T<sub>E</sub>X style file.